Laser Light Scattering Study of a Rigid-Rod Polyelectrolyte

Tianbo Liu,[†] Rudy Rulkens,[‡] Gerhard Wegner,[‡] and Benjamin Chu*[,†,§]

Department of Chemistry, State University of New York at Stony Brook, Stony Brook, New York, 11794-3400, Max-Planck-Institut für Polymerforschung, Postfach 3148, D-55021 Mainz, Germany, and Department of Materials Science and Engineering, State University of New York at Stony Brook, Stony Brook, New York, 11794-2275

Received March 17, 1998; Revised Manuscript Received June 5, 1998

ABSTRACT: Static light scattering (SLS), dynamic light scattering (DLS), and depolarized dynamic light scattering (DDLS) were employed to study methanolic solutions of an intrinsically stiff rigid-rod polyelectrolyte consisting of a poly(*p*-phenylene) backbone with dodecyl side chains. The solutions of the rigid rod polymers exhibit polyelectrolyte-solution properties at low counterion concentrations of tetramethylammonium chloride (TMACl). At higher salt concentrations, the single polymer molecules and the aggregates coexist in solution. The amount of aggregates varies with the polymer concentration and the nature of the counterions. By combining SLS with DLS studies, a new way of characterizing the basic parameters (such as the weight average molecular weight and the radius of gyration of the single polymer chains and the aggregation number of the aggregates) of the rodlike polyelectrolyte polymer chains in the presence of the corresponding aggregates has been presented. DDLS studies allowed for elucidation of the aggregated structures.

Introduction

In comparison with flexible random coil polymers, shear thinning and liquid crystalline properties of rigid-rod polymers have unique properties that allow for specialty applications. However, their characterization has always been a challenging problem because rigid-rod polymers tend to aggregate in solution. Intrinsically, rigid-rod polyelectrolytes are even more difficult to characterize in view of the presence of long-range electrostatic interactions.[1] Polymers with a poly(*p*-phenylene) backbone are intrinsically rigid rods due to the linear configuration of the phenylene repeat units. On the basis of the earlier work of Rulkens, Schulze, and Wegner,[2] the conjugated π-system was shown to provide interesting electrical and optical properties. Rehahn, Schlüter and Wegner[3,4] have developed the synthetic techniques to produce high molecular weight poly(*p*-phenylene) with a large variety of side groups.

The sulfonated poly(*p*-phenylenes) furnished with dodecyl side chains, a type of rigid-rod polyelectrolyte, synthesized by Rulkens et al.[2] have attracted particular interest. The backbone and dodecyl side chains of the sulfonated poly(*p*-phenylenes) are very hydrophobic and therefore tend to aggregate in strong polar solvents, e.g., water.[5] The precursor polymer where the sulfonate groups are esterified as arenesulfonate increases the solubility in nonpolar organic solvents, e.g., THF or toluene. The sulfonated groups can dissociate in polar solvents, resulting in the formation of a polyelectrolyte and thereby increasing the solubility. These opposing requirements, i.e., the dissociation of the ionogenic groups requires polar solvents while the hydrophobic backbone segments demand nonpolar solvents that can dissolve the phenylene-type backbones, thereby impose a serious restriction in finding a suitable solvent. Indeed, large aggregates could easily exist in aqueous solutions, even in the presence of added salt, which increased the ionic strength and shielded the electrostatic long-range interactions.[5] This difficulty prevents us from characterizing the poly(*p*-phenylenes) with dodecyl side chains in aqueous solution. The basic parameters of the polymers (such as the contour length, weight average molecular weight and the persistence length) were determined via their sulfonated ester precursors in THF and toluene.[6] The results showed that in these organic solvents, the sulfonated poly(*p*-phenylene) existed as wormlike chains, with a persistence length of 13 nm.

The characterization of intrinsically rigid rod polyelectrolytes in polar solvents is the objective of the present paper. Under the realization that in aqueous solution, an appreciable amount of aggregation would be unavoidable, we turn to nonaqueous polar solvents with a weaker polarity. We report the characterization of sulfonated poly(*p*-phenylene) in methanol, which has a high dielectric susceptibility by using a combination of static light scattering (SLS), dynamic light scattering (DLS), and depolarized dynamic light scattering (DDLS) measurements.

Experimental Section

Synthesis, Sample Preparation, and Previous Characterization. The synthesis of polymer P4, whose formula is shown in Figure 1a, has been reported elsewhere.[2,5] The sulfonate ester precursor of polymer P4 (Figure 1b) has a weight average molecular weight (M_w) of about 100k (actually 1.01×10^5 by light scattering) with a polydispersity index M_w/M_n of about 2, M_n being the number average molecular weight; also, it has the weight average contour length $\langle L_w \rangle$ of 122 nm, number average contour length $\langle L_n \rangle$ of 49 nm.[6] Different types of counterions, in the form of solution or TMA chloride, can be introduced by dialysis of the P4 polymer with appropriate salt solutions containing the desired counterions. The solvent is then removed by freeze-drying.

Methanol, ethanol, and butanol (grade HPLC, Fisher Chemical Corp.) were used without further purification. First, the polymer in its respective salt forms was dissolved in the

* To whom correspondence should be addressed.
[†] Department of Chemistry, State University of New York.
[‡] Max-Planck-Institüte für Polymerforschung.
[§] Department of Materials Science and Engineering, State University of New York.

S0024-9297(98)00423-9 CCC: $15.00
Published on Web 08/19/1998

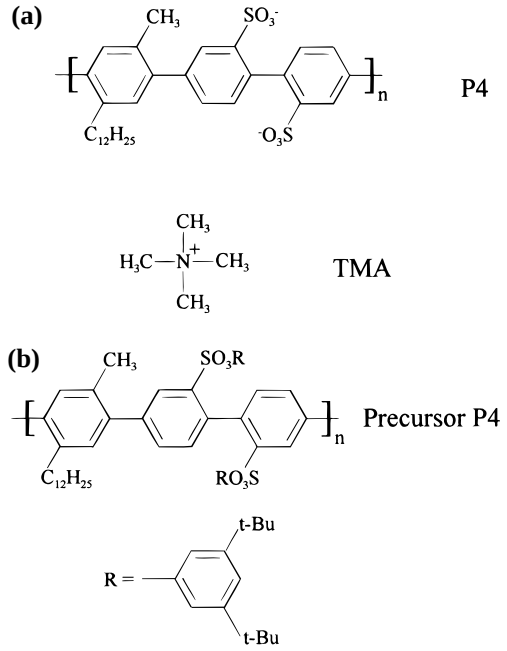

Figure 1. Chemical formula of a sulfonated poly(*p*-phenylene) (P4): (a) in the form of tetramethylammonium (TMA) salt; (b) precursor P4 polymer.

solvent. The solution was dialyzed for at least 1 day by using dialysis tubes (Pope Scientific, Inc., 6000−8000 Dalton) in order to guarantee the same ionic chemical potential for the solvent containing the counterions and the polymer solution.

SLS, DLS, and DDLS Measurements. The refractive index increments (dn/dc) of P4 solutions were measured by using a Brice-Phoenix differential refractometer. At 488 nm, the dn/dc of P4 in 0.01 M TMA in methanol was $(0.301 \pm 0.004) \times 10^{-6}$ mL/g. A standard, laboratory-built light scattering spectrometer with an argon ion laser operating at 488 nm was used for the scattering experiments. The instrument was capable of making measurements in the angular dependence both of the absolute integrated scattered intensity and of the photon correlation.[7] SLS experiments were performed at scattering angles between 30 and 140°, at 2° intervals. However, due to the large fluctuations in scattered intensities at low scattered angles, in the final analysis we removed the data from 30−40°. To ensure the high quality of the scattering curves, the measurements were repeated several times. Photon correlation measurements were made by means of a Brookhaven 9000 AT digital correlator. DLS measurements were performed at scattering angles of 45, 60, 90, 120, and 140°. An analyzer was placed in front of the photomultiplier tube (PMT) detector, to isolate either vertically or horizontally polarized light with respect to the scattering plane.

The basis for data analysis of SLS is the Rayleigh−Gans−Debye equation:[8]

$$Hc/R_\theta = 1/M_w(1 + q^2\langle R_g^2\rangle/3) + 2A_2c \quad (1)$$

with

$$H = 4\pi^2 n^2(\mathrm{d}n/\mathrm{d}c)^2/N_A\lambda_0^4 \quad (2)$$

$$q = (4\pi n/\lambda_0)/\sin(\theta/2) \quad (3)$$

where the Rayleigh ratio R_θ depends on the intensity of the scattered light (I) at different scattering angles θ, c is the polymer concentration, q is the magnitude of the scattering wave vector, $\langle R_g^2\rangle$ is the mean square radius of gyration of the particles, A_2 is the second virial coefficient, n is the refractive index of the solvent, N_A is the Avogadro constant, and λ_0 is the wavelength of incident light in a vacuum.

DLS measures the intensity−intensity time correlation function $G^{(2)}(\Gamma)$ by means of a multichannel digital correlator.[9]

$$G^{(2)}(\Gamma) = A(1 + b|g^{(1)}(\tau)|^2) \quad (4)$$

where A, b, and $|g^{(1)}(\tau)|$ are, respectively, the background, a coherence factor, and the normalized electric field time correlation function. The field correlation function $|g^{(1)}(\tau)|$ was analyzed by the constrained regularized CONTIN[10] method, to yield information on the distribution of the characteristic line width (Γ) from

$$|g^{(1)}(\tau)| = \int G(\Gamma)\mathrm{e}^{-\Gamma t}\mathrm{d}\Gamma \quad (5)$$

The normalized distribution function of the characteristic line width $G(\Gamma)$ so obtained can be used to determine an average apparent translational diffusion coefficient D_{app}

$$D_{app} = \Gamma/q^2 \quad (6)$$

The apparent hydrodynamic radius $R_{h,app}$ is related to D_{app} via the Stokes−Einstein equation:

$$R_{h,app} = kT/(6\pi\eta D_{app}) \quad (7)$$

where k is the Boltzmann constant and η is the viscosity of the solvent at temperature T. The average D_{app}, $\langle D_{app}\rangle$, as well as $\langle 1/R_{h,app}\rangle$, is a z-average value.[11,12] From DLS measurements, we can obtain the particle-size distribution in solution from a plot of $\Gamma G(\Gamma)$ versus $R_{h,app}$, with $\Gamma_i G(\Gamma_i)$ being proportional to the angular-dependent scattered intensity of particle i having an apparent hydrodynamic radius $R_{h,i}$. The relative peak area of each mode represents the contribution to the total scattered intensity due to that kind of particle.

DDLS measures the rotational diffusion coefficient (Θ) of the macromolecules.[13] By detecting the depolarized scattered intensity using vertically polarized incident light, I_{VH}, the CONTIN analysis yields a distribution of characteristic line width Γ_{VH}, with

$$\Gamma_{VH} = Dq^2 + 6\Theta \quad (8)$$

The magnitude of I_{VH} is related to the molecular anisotropy in solution. For solvated spheres,

$$\Theta = kT/(8\pi\eta a^3) \quad (9)$$

with a being the radius of the sphere.

Results and Discussion

Effect of Solvents. P4-TMA shows different solubility in different polar solvents. Generally, due to the very hydrophobic poly(*p*-phenylene) backbone and dodecyl side chains, large aggregates tend to form. Parts a and b of Figures 2 show, respectively, the CONTIN results of ~1.0 mg/mL P4-Na in water and in MeOH at $\theta = 90°$ in the presence of 0.01 M NaCl. Two modes were observed from solutions in water as well as in MeOH. The fast modes have values of $R_{h,app}$ of the order of 5−8 nm, with the size being a little smaller for aqueous solutions. They are attributed to the diffusive translational motions of (smaller) single polymer chains. The slow modes could be identified with the translational motions of the larger aggregates. It is clear that water is not a good solvent for P4-Na, because the aggregates from P4-Na with sizes in the range of 40−45 nm are mainly responsible for the observed scattered

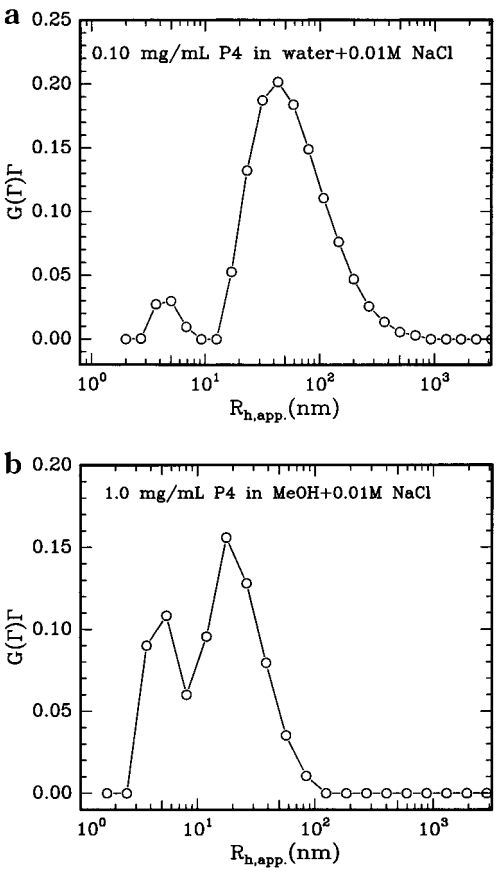

Figure 2. (a) CONTIN result of 0.10 mg/mL P4 (with Na^+ being the counterion) in water + 0.01 M NaCl. (b) CONTIN result of 1.0 mg/mL P4 (with Na^+ being counterions) in MeOH + 0.01 M NaCl.

intensity. In MeOH, the peak intensity areas of the two modes are comparable only when the polymer concentration is increased by a factor of 10, from 0.1 to 1.0 mg/mL, suggesting that, to disperse the P4 polymers, MeOH is a much better solvent than water, possibly due to its weaker polarity, which favors solvation of the hydrophobic part of P4. It is noted that at $c = 0.4$ mg/mL (figure not shown), a smaller intensity peak for the aggregates was observed. However, we were not able to obtain a unimodal size distribution at even lower polymer concentrations because the total scattered intensity then became too weak for a reasonable data analysis by the CONTIN method. The solubility of P4 in other kinds of aliphatic alcohols, such as ethanol and *n*-butanol, was also tested. They were better solvents than water, but not as good as MeOH. Therefore, only MeOH was chosen as the solvent in our study.

Effect of Different Counterions. Different counterions have proven to have a notable influence on the ionic interactions of polyelectrolytes. Larger counterions tend to enhance the solubility of the polyelectrolytes.[14] With Na^+ or TMA as the counterions, we see two modes according to the CONTIN results, as shown in Figure 2b and Figure 3. For the polyelectrolytes in the Na^+ salt form, the aggregates have a smaller size ($R_{h,app} = 25$ nm) than those in the TMA salt form ($R_{h,app} = 60$ nm). However, for example, at $\theta = 90°$, the peak area ratio (2.64:1) of the aggregates to that of the unimers in the former case (Na^+) is higher than that (1.53:1) in the latter case (TMA). Considering that the smaller particles have a much smaller scattering strength, we can conclude that the P4 molecules form a larger amount of smaller aggregates, with Na^+ being the counterions than with TMA being the counterions.

TMA was selected as the counterion for further studies because the two peaks in the CONTIN results are totally separated, making it feasible to *estimate* the unimer and aggregate contributions from the total scattered intensity.

Effect of Co-ion Concentration. The co-ions (added salts) play an important role in determining the solution behavior of polyelectrolytes. Without co-ions, the charges on the polymer chains cannot be shielded effectively. Abnormal and unique phenomena for polyelectrolytes could be observed in light scattering measurements.[15,16] Higher co-ion concentrations lower the effective charge density on the polymer chains and thereby decrease the polymer solubility. At high enough co-ion concentrations the polyelectrolytes could be precipitated due to the salting out effect.

The nature of the two modes at low co-ion concentrations is still under discussion. The more accepted explanation for the slow mode is that it is caused by the long-range interactions among the polyelectrolytes,[15,16] and not by the existence of real aggregates. In the "Temporal aggregate" (TA) model,[17,18] presented in the early 1980s, the local concentration fluctuations were related to the long-range electrostatic interactions in solution. Some authors suggested that the slow mode was simply due to "filterable aggregates".[19−22]

A common observation of the slow mode is shown in Figure 4. At low salt concentrations (0.005 M NMe_4-Cl), the apparent R_h values ($R_{h,app}$) of the slow mode increase with increasing scattering angle, which is abnormal when compared with $R_{h,app}$ values of neutral polymers in solution. At low salt concentrations, the charges on the polymer backbone cannot be effectively shielded. A similar phenomenon has been reported by Ito et al.[23] who found that, for the PMMA latex/water system, the curve of D_p^0/D_{app} versus q exhibited a couple of maximums. They suggested some form of structural ordering in the solution, with D_p^0 being the translational diffusion coefficient at the infinite dilution limit. Three possible interpretations have been presented:[24] the correlation hole, the "two-state" structure of polyion solutions, and the TA model.

On the contrary, at higher salt concentrations (0.01 M), the $R_{h,app}$ value of the slow mode decreases with increasing scattering angle. The charges on the polyelectrolyte chains are shielded and the slow modes as shown in Figures 2 and 3 are likely to be related to real aggregates. Our data analysis, however, does not depend on the details of the nature of the slow mode.

With further increase in the salt concentration, the solubility of the polyelectrolytes in polar solvents is decreased. Finally, at salt concentrations beyond 0.05 M TMACl, the salting out effect occurs for P4-TMA in MeOH.

4. Aggregation Behavior of P4 at 0.01 M TMACl Concentration. A salt concentration of 0.01 M TMACl was chosen for detailed studies. The reason is that this concentration is high enough to shield the electrostatic interactions among the charged polyelectrolyte chains, as illustrated by Figure 4, but sufficiently low to avoid the salting out effect. Furthermore, from preliminary screening, the intensity contributions to the total scattered intensity due to the two modes are comparable so that we can isolate the two contributions for independent analysis of single P4 chains and their aggregates.

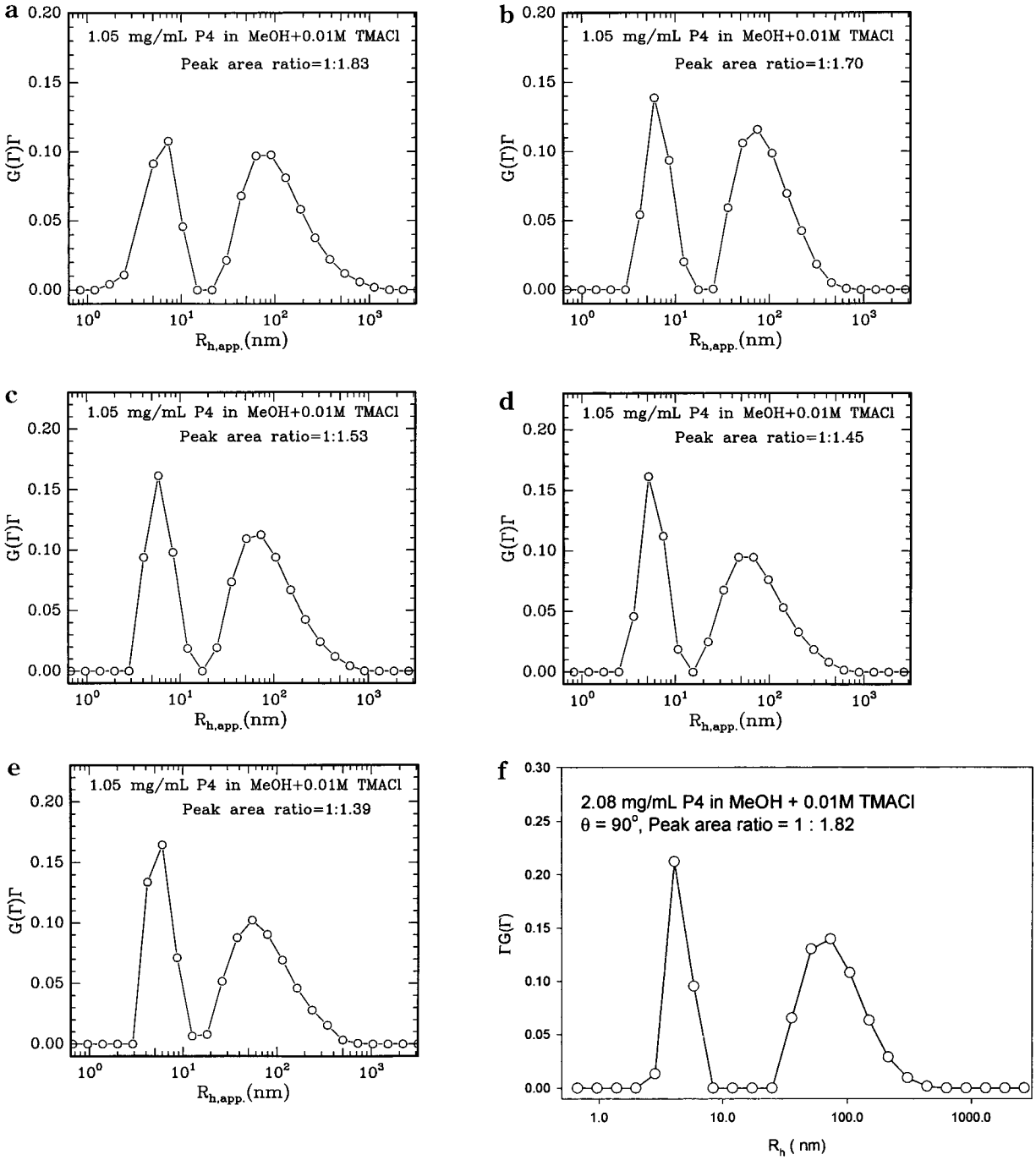

Figure 3. CONTIN results of 1.05 mg/mL P4 (with TMA being the counterion) in MeOH + 0.01 M TMACl at different scattering angles: (a) 45°; (b) 60°; (c) 90°; (d) 120°; (e) 140°. (f) 2.08 mg/mL P4 (with TMA being the counterion) in MeOH + 0.01 M TMACl at 90°.

The traditional way to analyze SLS data is to use the Zimm plot. However, the normal Zimm plot is not so useful as our main objective is to characterize the single chain polyelectrolyte. For this special complex system, (1) the unimers coexist with large aggregates over the entire range of polymer concentrations we have studied and (2) the percentage of polyelectrolyte chains that form aggregates increases with increasing total polymer concentration.

Therefore, a usual Zimm plot can only provide the information of the polymer mixture containing both the unimers and the aggregates. Here we present a new way to characterize this polyelectrolyte system by combining SLS and DLS results.

SLS measurements were repeated several times to get the angular dependence of the total scattered intensity, as shown in Figures 5 and 6. DLS measurements allow for the estimation of the relevant scattered intensity ratio of the two different modes that we shall refer to as species from here on. Typical scattering profiles are shown in Figure 3a−e, for 1.05 mg/mL P4-TMA in MeOH with 0.01 M TMACl. The peak area ratio of the unimers to that of the aggregates increases with increasing scattering angle, from 1:1.8 at 45° to 1:1.4 at 140°, with the error limits to the area ratio of the order of 0.1. The total scattered intensity at each scattering angle represents the summation of the scattered intensity due to the unimers and the aggregates. The

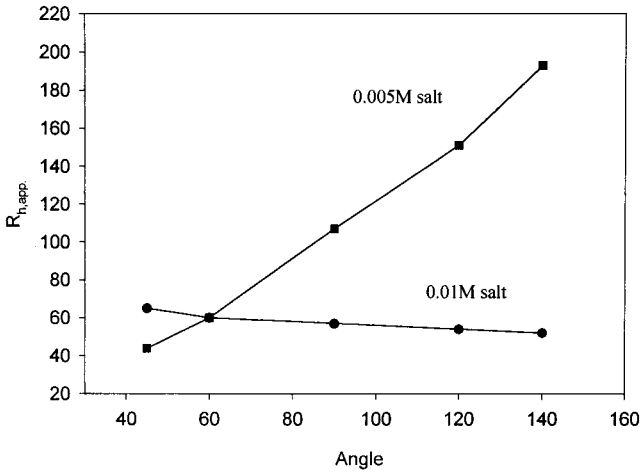

Figure 4. Angular dependence (q dependence) of $R_{h,app}$ of 1.05 mg/mL P4 (with TMA being the counterion) in MeOH + 0.005 M TMACl (filled circles) and in MeOH + 0.01 M TMACl (filled squares).

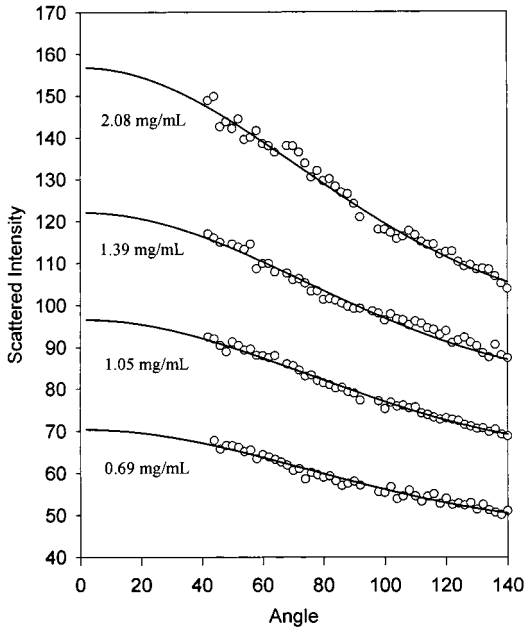

Figure 5. Comparison of theoretical (solid curves) and experimental (open circles) results on the scattering curves of P4 (with TMA being the counterion) at various P4 concentrations in MeOH + 0.01 M TMACl.

fraction of the scattered intensity due to the two different species could be estimated as the ratio of the peak areas based on the CONTIN analysis. Therefore, the scattered intensity due to the unimers and the aggregates at each scattering angle can be separated and estimated, as shown in Figure 6. The details are described in the following paragraphs. Similar procedures were used for data obtained at different polymer concentrations, as shown in Figure 5. At higher polymer concentrations, the peak area due to the aggregates occupied a higher percentage of the total scattered intensity. However, the R_h values of the two species remained similar to those values at lower polymer concentrations, as shown for example in Figure 3f in comparison with Figure 3a−e at two different polymer concentrations.

Although we cannot determine the percentage amount of the P4-TMA molecules that are in aggregated states for a given concentration, we can analyze the data if

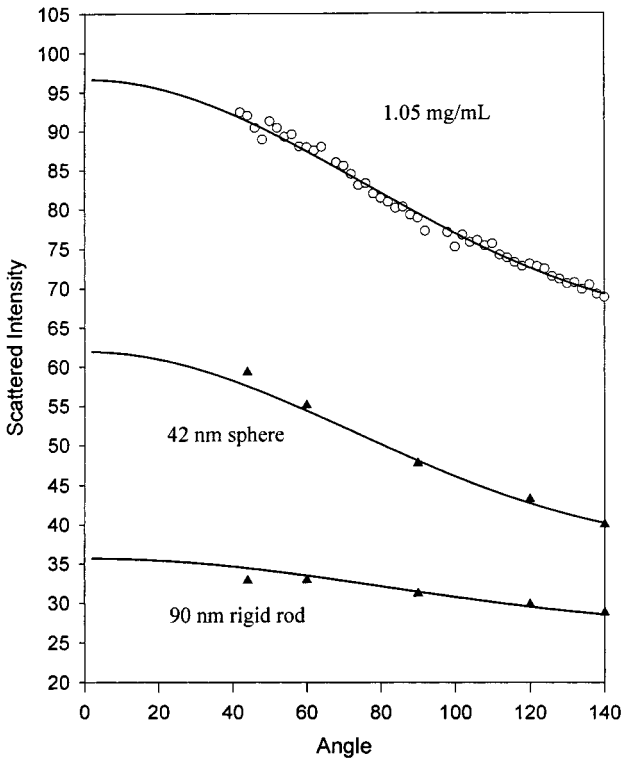

Figure 6. Decomposition of theoretical (solid curves) and experimental (open circles) results on the scattering curves of 1.05 mg/mL P4 (with TMA being the counterion) in MeOH + 0.01 M TMACl. The experimental filled triangles were calculated by combining SLS and DLS measurements. The details are presented in the text.

the aggregation process follows a closed association mechanism where there exists a critical micelle concentration (cmc). With the assumption that the unimer concentration is maintained at the cmc for polymer concentrations slightly above the cmc, the analysis can be much simplified.[25] In the present case, we have no evidence for the existence of such a critical micelle concentration. Therefore, some assumptions and fitting with theoretical models are needed to analyze the above data. The approach is described as follows.

The scattered intensity of particles is determined by the form factor $P(q)$ and the structure factor $S(q)$:

$$I(q) \propto P(q)\, S(q) \tag{10}$$

$P(q)$ is determined mainly by the size and the shape of the particles in solution, and $S(q)$ is related to the interparticle interactions, which are related to the polymer concentration c by[26]

$$\varphi = (4\pi R_{HS}{}^3/3) N_A c/M \tag{11}$$

with φ being the volume fraction of the equivalent hard spheres, R_{HS} being the radius of the equivalent hard sphere, and M being the molar mass of the particle. At low polymer concentrations (c < 2.1 mg/mL), the magnitude of the φ value is very small (≈0.01) and therefore we can assume $S(q) = 1$ without introducing large errors. Therefore, only the $P(q)$ term should be considered. At each polymer concentration, the scattered intensity due to the unimers shows a very weak angular dependence (Figure 6) and can be approximated by a long, thin rigid rod, which is a reasonable assumption based on the geometrical nature of the polymer chains.

However, due to the pronounced angular dependence of the experimental scattering curve, the intensity contributions for the aggregates require a more complex approach. The purpose of this fitting is to make a reasonable extrapolation of scattering curves to zero scattering angle so that the experimental data due to the single P4 chains (or unimers) and the aggregates can be effectively interpreted by known equations.

The effect of polydispersity should also be taken into account. It is relatively trivial for unimers because of the weak angular dependence of the scattered intensity. However, for the aggregates, the polydispersity effect could play a noticeable role in determining the overall scattering curve. From DLS measurements, the size distribution of the particles can be calculated by using the variance $\mu_2/\bar{\Gamma}^2 \approx 0.3$ for the aggregates with $\mu_2 = \int(\Gamma - \bar{\Gamma})^2 G(\Gamma)\, d\Gamma$ and $\bar{\Gamma} = \int \Gamma G(\Gamma)\, d\Gamma$. The CONTIN analysis reveals a *z*-average distribution for R_h while we are fitting the curves by using a number-average Gaussian distribution from DLS, as shown in Figure 3. The difference in the weighting factor can be correlated. For polydisperse particles, the normalized number-average molecular weight distribution [$F_n(M)$] is related to the normalized weight-average molecular weight distribution [$F_w(M)$]:[27]

$$F_w(M)/F_n(M) = M/M_n \tag{12}$$

with M_n being the number-average molecular weight. The relation between $F_w(M)$ and M has been presented by Zhou et al.:[12]

$$F_w(M) \propto G(D)D/M^2 \propto G(D)D^{1+2/\alpha_D} \tag{13}$$

where $G(D)$ is the normalized distribution of D and $G(D)D$ is proportional to $G(\Gamma)\Gamma$ in the CONTIN analysis. α_D is related to the expression

$$D = k_D M^{-\alpha_D} \tag{14}$$

where k_D is another parameter. The value of α_D is related to the polymer conformation. For spheres, $\alpha_D = {}^1/_3$, and therefore we can calculate the number-average size distribution of the particles from the above expressions. For the aggregates, the calculated number-average radius for spheres with a uniform density is about 38 nm by using an equivalent Gaussian distribution $G(r)$ for the aggregates:

$$G(r) = 1/N \exp[-(r - r_0)^2/2\sigma^2] \tag{15}$$

where r is the particle radius, r_0 (=38 nm, in this case) is the peak position, N is a normalization factor, and σ represents the broadness of the size distribution, which is related to the half-height at half-width of the distribution peak based on Figure 3a. Relevant parameters including upper and lower limits of the size distribution can be estimated from DLS measurements. The scattering curves due to the P4 aggregates can be fitted quite well by using the polydisperse solid spheres model having a Gaussian size distribution (eq 15) and a number average radius R of 42 nm, as shown in Figure 6 where we have now adjusted the peak position in eq 15 in order to best fit the total scattering curve. In the presence of polydispersity for the aggregates, the form factors for the unimers and the aggregates have the form[24]

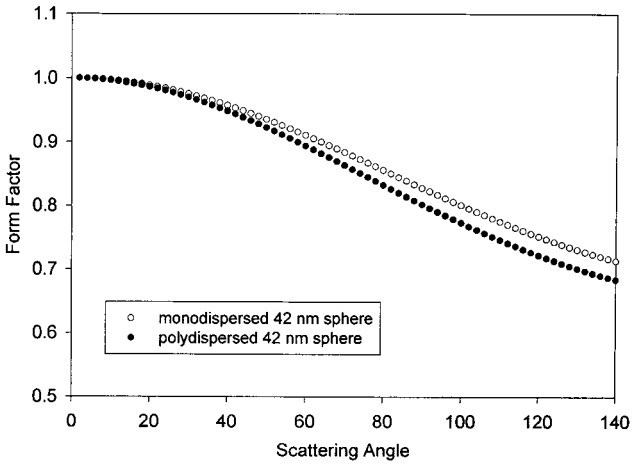

Figure 7. Effect of polydispersity on the scattering curve having a 42-nm radius sphere. The polydispersed scattering curve is based on eqs 15 and 17 with $\sigma = 12$ nm, $r_0 = 42$ nm, and $\lambda_0 = 488$ nm.

unimers (based on the rigid rod model)

$$P(qL) = (2/qL)\int_0^{qL}(\sin Z/Z)\, dZ - [(2/qL)\sin(qL/2)]^2 \tag{16}$$

aggregates (based on the solid sphere model)

$$P(qR) = 1/(N\upsilon)\int_a^b [3/(qR)^3\{\sin(qR) - (qR)\cos(qR)\}]^2 \exp[-(r - R)^2/2\sigma^2]\, dr \tag{17}$$

where L is the length of the rigid-rod unimers and a and b represent the lower and upper size boundaries of the aggregates estimated from a combination of DLS measurements and CONTIN analysis. The normal Gaussian distribution has boundaries of positive and negative infinities. However, in our case, we have finite boundaries. Therefore, a normalization factor υ is introduced to guarantee the integration of the total peak area to be unity.

Figure 7 shows the calculated scattering curves for 42-nm radius equivalent spheres with (hollow circles) and without (filled circles) polydispersity. Figure 6 shows an example for the superposition of two scattering curves: the lowest curve represents a rigid rod model with a rod length $L_{rod} = 90$ nm for the unimers and the middle one is for an equivalent 42-nm radius sphere model in the presence of polydispersity. The filled circles represent the experimental data on the basis of SLS measurements at 1.05 mg/mL P4-TMA concentration. The filled triangles represent the measured scattered intensities of the unimers and of the aggregates by combining SLS and DLS experiments. The ratios of the scattered intensity from the two theoretical curves can be scaled by using the intensity ratios obtained from the Laplace inversion of the electric field correlation function (Table 1). The calculated total scattering curve (the highest curve with open circles) can be effectively superimposed to the experimental data (filled circles). Similar fittings were performed to the scattering curves at other polymer concentrations (0.69, 1.39, and 2.08 mg/mL), as shown in Figure 5. The aggregates at all of the concentrations can be fitted by using the equiva-

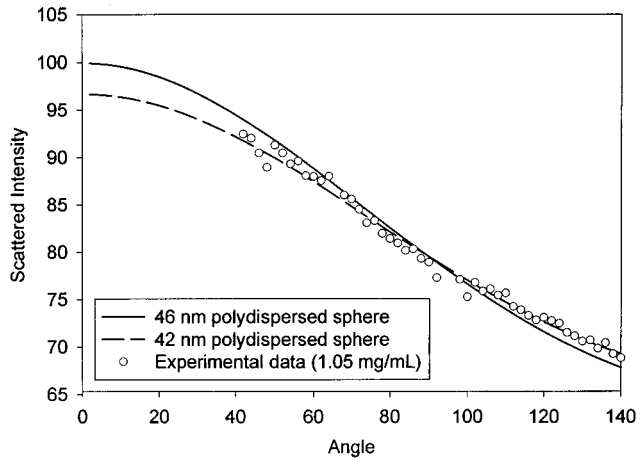

Figure 8. Fitting of experimental data with 42-nm and 46-nm polydispersed spheres.

Table 1. Calculated and Measured Peak Area Ratios of Aggregates and Unimers at Different Scattering Angles (2.08 mg/mL P4 + 0.01 M TMACl in Methanol)

scattering angle (deg)	45	60	90	120	140
measd peak area ratio (A_{agg}:A_{uni}) (±0.1)	1.83	1.70	1.53	1.45	1.39
calcd peak area ratio (A_{agg}:A_{uni})	1.79	1.68	1.53	1.45	1.40

lent 40−42-nm radius polydisperse sphere model, radii which are similar to the calculated value of 38 nm based on Figure 3a alone.

The accuracy of this fitting can be tested by making small variations in the fitting parameter. In Figure 8, the computed scattering curve in Figure 6 for the aggregates was also plotted by using $R = 46$ nm. It is obvious that the fitting curve with $R = 46$ nm has shifted away from the experimental data. Depending on the accessible q-range, the plot also provides us with an experimental uncertainty based on our very approximate model. It is clear that the aggregates are not likely to be polydisperse spheres. However, we shall show that on the basis of the experimental q-range investigated the results are essentially independent of this assumption.

Although the spherical model can fit the scattering curves of the aggregates quite well, the result from DDLS measurements has led us to consider whether it is a reasonable model for describing the aggregates. The P4-TMA/MeOH solution with 0.01M TMACl has an I_{VH}/I_{VV} value of about 3.5%, where I_{VH} and I_{VV} are, respectively, the polarized and depolarized scattered intensities by using an incident polarized light. With a photon correlation experiment of over 24 h for one DDLS intensity time correlation function curve, the CONTIN analysis yielded only one broad peak, respectively, for 1.39 and 2.08 mg/mL P4 solutions, with an average G_{VH} value of about 1.33×10^4 s^{-1} at $\theta = 140°$, while under the same experimental conditions, the Γ_{VV} value of the aggregates was of the order of 5.65×10^3 s^{-1}. If we take the z-average $R_{h,app}$ of the aggregates to be 60 nm, from eq 9 we can get the z-average rotational diffusion coefficient of the aggregates $\theta_{agg} = 1.22 \times 10^3$ s^{-1}. At the same time, by using eq 8, $\theta_{agg} = (\Gamma_{VH} - \Gamma_{VV})/6 = 1.29 \times 10^3$ s^{-1}. This coincidence in θ_{agg} value indicates that the characteristic line width in the DDLS measurement was indeed due to the aggregates. We can also estimate the θ_{uni} value from the $R_{h,app}$ value of the unimers according to eq 9, $\theta_{uni} \approx 1 \times 10^6$ s^{-1}, too fast to be detected by our current instrumental setup.

The existence of I_{VH} due to the aggregates cannot be explained by using a spherical model, because for a sphere, I_{VH} should be equal to zero. On the other hand, since the unimers are rigid-rod molecules, it is not expected that they form spherical shape aggregates by random looping and bending. Therefore, it is reasonable to consider another model: the cylinder model. Again, the size of the cylinder can be obtained from the equivalent R_h value through the DLS measurements. The size of an equivalent cylinder can be calculated by using the following relation:[24]

$$R_h/R_S = (2/3)^{1/3} p^{2/3}/\ln p \qquad (18)$$

where $p = L/2R_c$, with L and R_c being the length and the radius of the cylinder; R_S is the radius of the equivalent sphere which has the same volume as the cylinder. It means that for a cylinder and a sphere that have the same volume, the R_h value of the cylinder will be larger. There are two parameters for a cylinder (L and R_c). From the R_h value we can determine one if the other is known. Thus, the scattering curves of a set of cylinders having the same R_h values as the 42-nm polydispersed sphere can be created by using the expression below:[28]

$$P(q) = \int_0^{\pi/2} (9/2) \sin^2[qL \cos(\theta/2)]/(q^2L^2 \cos 2\theta) \times 4[J_1^2(qR_c \sin\theta)]/(q^2 R_c^2 \sin^2\theta) \sin\theta \, d\theta \qquad (19)$$

with J_1 being the first-order Bessel function and $J_1(x) = \sin x/x^2 - \cos x/x$.

To estimate the effect of polydispersity, a proper assumption on the conformation of the cylinder needs to be made in order to avoid cumbersome calculations. There are two basic conditions:

1. All the cylinders have the same radius but different length; i.e., the size difference which is reflected in a three-dimensional spherical model is again reduced to one dimension. It is quite easy to calculate that in this case, the longest chain will be nearly 200 times longer than the shortest chain over the same R_h range. This kind of head-to-head aggregation seems to be unlikely.

2. We assume that for all the cylindrical aggregates, the ratio of the length to the radius remains constant, i.e., the aggregates have a similar shape but different sizes. By using this assumption, the scattering curves of the cylinders with different L/R_c ratios can be calculated. From the set of calculated scattering functions, we can pick up the one that best fits the experimental curves (i.e., most similar to that of the equivalent sphere with a 42-nm radius), as shown in Figure 9. The best pair has $L = 90$ nm and $R_c = 30.8$ nm. This scattering curve is quite similar to that of the 42-nm radius sphere, demonstrating that the two fitting models can yield similar results over the entire light scattering range.

Based on the above model analysis, the scattered intensity at zero scattering angle for both the unimers and the aggregates can be estimated at each concentration. Now the concentration ratio of the unimers and the aggregates at each polymer concentration must be obtained so that we can obtain the information such as the polyelectrolyte molecular weight M_w and the aggregation number n_w at dilute polymer concentrations. An attempt has been made as follows:

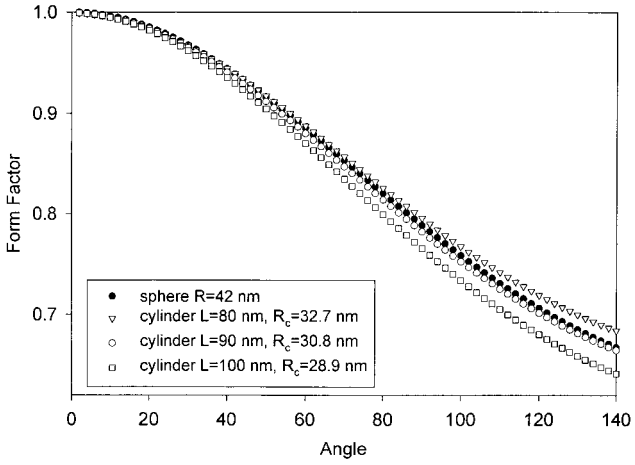

Figure 9. Scattering curves of different polydispersed cylinders having $R_{h,0} = 42$ nm (open symbols) and of polydisperse 42-nm spheres.

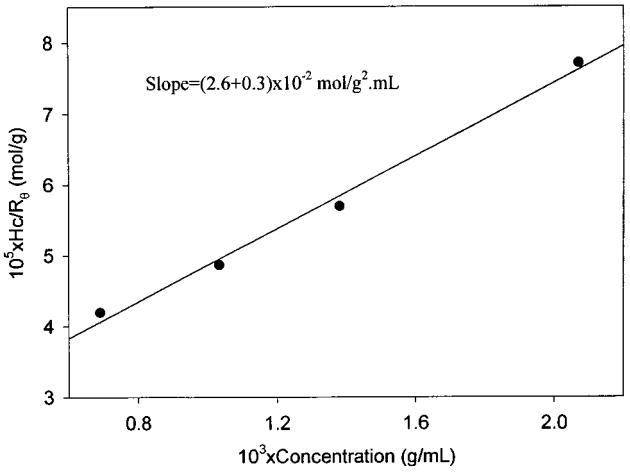

Figure 10. Plot based on eq 22 in order to estimate the $A_{2,uni}$

By considering the scattering data at four polymer concentrations, $c_{1,tot.}$, $c_{2,tot.}$, $c_{3,tot.}$, and $c_{4,tot.}$, and the relevant four total scattered intensities extrapolated to zero scattering angle, I_1, I_2, I_3, and I_4, obtained by SLS measurements and, also, by assuming the n_w of the aggregates to be constant at dilute polymer concentrations (≤2.08 mg/mL), as has been demonstrated by the fact that the aggregates at all the P4 concentrations can be fitted by using the 40−42-nm radius sphere model including the polydispersity effect, we get

$$Kc_{n,uni}/I_{n,uni} = 1/M_w + 2A_{2,uni}C_{n,uni} \quad (20)$$

$$K(c_{n,tot.} - c_{n,uni})/I_{n,agg} = 1/(n_w M_w) + 2A_{2,agg}(c_{n,tot.} - c_{n,uni}) \quad (21)$$

with $K = 4\pi^2 n^2 (dn/dc)^2 I_{Bz}/(R_{Bz} N_A \lambda^4)$, and $c_{n,uni}$ ($n = 1-4$) being the unimer concentration at polymer concentration $c_{tot.}$ (g/mL). There are eight equations and eight unknown parameters: $c_{1,uni}$, $c_{2,uni}$, $c_{3,uni}$, $c_{4,uni}$, the second virial coefficients of the unimers and the aggregates $A_{2,uni}$ and $A_{2,agg}$, M_w, and n_w. Theoretically, a solution exists. However, in practice, it is difficult to solve such a problem. Reasonable simplifications are introduced in order to obtain a plausible answer. It is noted that although the exact number concentration for the unimers is not known, it should be much larger than that of the aggregates, since we have selected a solvent MeOH that yields two intensity modes of comparable strength but quite different sizes. In addition, although the ratio c_{uni}/c is not a constant at different polymer concentrations, the difference can be quite small (e.g., about 90 wt % of unimers over the concentration range of our studies (>0.69 and <2.1 mg/mL)). Thus we can use the classical Rayleigh−Gans−Debye equation (eq 1) to plot a line:

$$Hc_{tot.}/R_\theta = B + 2A_2 c_{tot.} \quad (22)$$

where B is the offset. The molecular weight calculated from the B value is meaningless, because $c_{tot.} = c_{uni} + c_{agg}$. However, from a plot of Hc/R_θ versus polymer concentration ($c_{tot.}$), as shown in Figure 10, we can calculate the A_2 value from the slope and treat it as $A_{2,uni}$ without introducing large errors. With the measured refractive index increment (dn/dc) at 25 °C for this system, $(0.301 \pm 0.003) \times 10^{-6}$ mL/g at $\lambda_0 = 488$ nm, the calculation becomes easier with the results shown as follows:

$$A_{2,uni} = (1.3 \pm 0.2) \times 10^{-2} \text{ mol cm}^3/\text{g}^2$$

$$A_{2,agg} = (4.5 \pm 0.8) \times 10^{-3} \text{ mol cm}^3/\text{g}^2$$

$$M_w(\text{unimer}) = (4.8 \pm 0.8) \times 10^4$$

$$n_w = 16 \pm 3$$

and for all the concentrations, 87−92 wt % of the polyelectrolytes exist as single molecules.

It is noted that the cross-term for A_2 is neglected because of low polymer concentration. In the present case, we have separated the excess scattered intensity those due to the unimers and to the aggregates and have ignored the explicit interaction term between them, as the amount of aggregates was very small when compared with that of the unimers.

In our analysis, there are many steps in the fitting procedure. In addition, assumptions have been made to arrive at the above results. We can estimate the error limits as follows: from SLS measurements, ±3%; from DLS measurements to get the peak area intensity ratio, ±5%; from the (dn/dc) measurement, ±1−2%; from the fitting and extrapolation of the scattering curves to zero scattering angle: ±3%; from the calculation of $A_{2,uni}$: ±8−10%. Therefore, the total error on M_w and n_w is estimated to be of the order of 20% to 30%.

The precursor polymer[6] measured at the Max Planck Institute in Mainz had a weight-average molecular weight value of about 9.0×10^4. It is noted that the P4 polymer corresponds to P5 in reference 6. By subtracting the contribution due to the ester groups, the equivalent molecular weight for the P4 polymer chain was estimated to be about 5.4×10^4, which is about 10% higher than the present value. This discrepancy is within our estimated error limits. Nevertheless, we could also explore another source that could account for the difference: the P4-TMA polyelectrolytes form some kind of cylindrical aggregates whose conformation is beyond the range of the present method. The longer rodlike polymer chains are likely to be more hydrophobic and have a stronger tendency to form cylindrical micelles that in turn form the secondary aggregates. It then becomes possible that within the equilibrium between unimers and aggregates, statistically more of

the longer polymer chains are in the aggregates. Therefore, the measured molecular weight of the remaining polymer chains should be smaller.

The radius of gyration (R_g) of the unimers can be calculated from the scattering curves (the triangles in Figure 6), yielding a value of 25 ± 4 nm. If the unimers really exist as rigid rods, the total length should be equal to about 100 nm, with an equivalent R_g value of about 29 nm. Therefore, within the experimental error limits, it is reasonable to assume that the unimers exist as stiff but not truly rigid rods. From DLS measurements, the unimers had a $R_{h,0}$ value of 7−8 nm. Thus, the ratio of R_g/R_h is over 3, which is typical for stiff rods.

It should be noted that there is another apparently simpler way to analyze the data, i.e., by plotting a normal Zimm plot, the apparent average R_g of all the particles in solution, $R_{g,av}$ can be calculated. Then, by using the CONTIN results, the $R_{g,uni}$ and $R_{g,agg}$ can be calculated by using equations similar to eqs 20 and 21. However, this approach requires an assumption that $R_{g,av}$ is a constant at all polymer concentrations; i.e., the contributions to the total scattered intensity due to the unimers and the aggregates do not change with polymer concentration. That condition was not satisfied with our system, especially at higher polymer concentrations, as shown in Figure 3. The finer details require us to use a more general scheme for the present system, as we have presented.

As mentioned above, we have attributed the scattered intensity I_{VH} in DDLS measurements mainly to the aggregates. However, from the fitting results, the shape of the aggregates did not show a very large anisotropy. One of the explanations is that the I_{VH} value comes partly from the optical anisotropy in the aggregates, i.e., in the aggregates, the polyelectrolyte chains tend to choose the same direction and to form a bunch of aligned structures. The aligned structures have been shown to exist for the same polymer in aqueous solution by using small-angle X-ray scattering measurements.[20] In the current system, SAXS only gave very weak scattering curves without any characteristic peaks. The difference may be attributed to the nature of the solvents. In MeOH, as the majority of the P4-TMA molecules are unimers, no definitive structural information of the aggregates in solution can be obtained.

Conclusions

The rigid-rod polymer P4, which consists of a poly(*p*-phenylene) backbone furnished with charged sulfonate and nonpolar dodecyl side chains, was characterized by using laser light scattering (SLS, DLS, DDLS) in methanol in the presence of 0.01 M TMACl. P4 was also characterized in methanol over a range of salt concentrations.

Due to the hydrophobic backbone and dodecyl side chains, the P4 molecules tend to form aggregates in polar solvents. It was found that they could be dissolved better in methanol than in water. The type and concentration of the added salt also played a noticeable role in the polyelectrolyte aggregation behavior. P4-TMA showed typical properties of polyelectrolytes in methanol at low salt concentrations that can be avoided at higher salt concentrations. Salting-out was found at higher salt concentrations.

Theoretical models were employed to fit the data from SLS and DLS measurements. The scattering curves of the unimers could be fitted well by assuming a long, thin rod. The scattering profile of the aggregates could be represented by either solid spheres or, more realistically, by cylinders. By extrapolation of the fitted curves to zero scattering angle, the parameters of the single molecules and of the aggregates were calculated. The calculated M_w obtained this way was a little smaller than the value obtained from the precursor polymers. Nevertheless, the agreement could be considered to be excellent, especially if one were to take into account the equilibrium between the unimers and the aggregates, together with the nature of the aggregates. The aggregation number of the aggregates was about 16. The large positive values of A_2 for the unimers and the aggregates indicated the strong repulsive interactions among the polyelectrolyte chains. The methodology illustrates that we have developed an analytical method to characterize rodlike polyelectrolytes in solution in the presence of a small amount of large aggregates.

The I_{VH} was attributed to the aggregates, and suggested some degree of intrinsic anisotropy. On the basis of the results of the same polymer in water, the optical anisotropy could be attributed to the aligned structures of cylindrical micelles in the aggregates.

Acknowledgment. B.C. gratefully acknowledges support of this work by the National Science Foundation (DMR9612386) and the Department of Energy (DEFG0286ER45237.012). T.L. thanks Dr. Kenneth S. Schmitz for his kind help in providing the necessary mathematical equations.

References and Notes

(1) Chu, B.; Ying, Q.; Wu, C.; Ford, J. R.; Dhadal, H. S. *Polymer* **1985**, *26*, 1408.
(2) Rulkens, R.; Schulze, M.; Wegner, G. *Macromol. Rapid Commun.* **1994**, *15*, 669.
(3) Rehan, M.; Schlüter, A.-D.; Wegner, G. *Polymer* **1989**, *30*, 1060.
(4) Schlüter, A.-D.; Wegner, G. *Acta Polym.* **1993**, *44*, 59.
(5) Rulkens, R. Ph.D. dissertation, Max-Planck-Institut für Polymerforschung, Mainz, Germany, 1996.
(6) Vanhee, S.; Rulkens, R.; Lehmann, U.; Rosenauer, C.; Schulze, M.; Kohler, W.; Wegner, G. *Macromolecules* **1996**, *29*, 5136.
(7) Zhou, Z.; Chu, B. *J. Colloid Interface Sci.* **1988**, *126*, 172.
(8) Hiemenz, P. C. *Principle of Colliod and Interface Chemistry*; Marcel Dekker: New York, 1985.
(9) Chu, B. *Laser Light Scattering*; Academic Press: New York, 1991.
(10) Provencher, S. W. *Biophys. J.* **1976**, *16*, 29; *J. Chem. Phys.* **1976**, *64* (7), 2772.
(11) Wu, C.; Zuo, J.; Chu, B. *Macromolecules* **1989**, *22*, 633.
(12) Zhou, S.; Fan, S.; Au-Yeung, S. C. F.; Wu, C. *Polymer* **1995**, *36*, No. 7, 1341.
(13) Pecora, R., Ed. *Dynamic Light Scattering*; Plenum Press: New York, 1985; p 66.
(14) Oosawa, I. *Polyelectrolytes*; Chemistry-Microphase-International: 1988; Chapter 4.
(15) Schmitz, K. *Macroions*; Solution and Colloidal Suspension; VCH Publishers: Deerfield Beach, FL, 1993.
(16) Sedlak, M.; Amis, E. J. *J. Chem. Phys.* **1992**, *96*, 826.
(17) Schmitz, K.; Lu, M.; Singh, N.; Ramsay, D. J. *Biopolymers* **1984**, *23*, 1637.
(18) Ramsay, D. J.; Schmitz, K. *Macromolecules* **1985**, *18*, 2422.
(19) Reed, C. E.; Li, X.; Reed, W. F. *Biopolymers* **1989**, *28*, 1981.
(20) Ghosh, S.; Li, X.; Reed, C. E.; Reed, W. F. *Biopolymers* **1990**, *30*, 1101.
(21) Li, X.; Reed, W. F. *J. Chem. Phys.* **1991**, *94*, 4568.
(22) Norwood, D. P.; Benmouna, M.; Reed, W. F. *Macromolecules* **1996**, *29*, 4293.
(23) Ito, K.; Okumura, H.; Yoshida, H.; Ueno, Y.; Ise, N. *Phys. Rev. B* **1988**, *38*, 10852.

(24) Schmitz, K. S. *An Introduction to Dynamic Light Scattering by Macromolecules*; Academic Press: New York, 1990.
(25) Liu, T.; Zhou, Z.; Wu, C.; Chu, B.; Schneider, D. K.; Nace, V. M. *J. Phys. Chem. B* **1997**, *101*, 8808.
(26) Vrij, A.; Jansen, J. W.; Dhont, J. K. G.; Pathmamanoharan, C. *Faraday Discuss. Chem. Soc.* **1983**, *76*, 19.
(27) Munk, P. *Introduction to Macromolecular Science*; John-Wiley & Sons: New York, 1989; Chapter 1.
(28) Guinier, A.; Fournet, G. *Small-angle Scattering of X-rays*; Wiley: New York, 1955.

MA980423+